Journal of Materials Chemistry B

Accepted Manuscript

ROYAL SOCIETY OF CHEMISTRY

www.rsc.org/materialsB

Journal Name

ARTICLE

An integrin-targeting nanosystem as the carrier of selenadiazole derivative to induce ROS-mediated apoptosis in bladder cancer cells, from rational design to action mechanisms†

Received 00th January 20xx,
Accepted 00th January 20xx

DOI: 10.1039/x0xx00000x

www.rsc.org/

Yifan Wang,[a] Wenying Li,[a] Yahui Yang,[a] Qinsong Zeng,[b] Ka-Hing Wong[c,d], Xiaoling Li,*[a] and Tianfeng Chen *[a]

The development of novel therapeutics for patients with bladder cancer is an important area of research, particularly considering the rather limited treatment options currently available. In this study, we designed and synthesized a conjugate of the cancer-targeting selenadiazole derivative BSeC (benzo [1, 2, 5] selenadiazole-5-carboxylic acid) and the RGD (arginine-glycine-aspartate) peptide, which was used as targeting molecule, using a PEI polymer as a linker. The results showed that BSeC-PEI-RGD formed core-shell spherical nanoparticles with improved stability in physiological and low pH solutions. The cancer-targeting design significantly enhanced cellular uptake of BSeC-PEI-RGD and decreased its cytotoxicity to normal cells. The nanoparticles could inhibit the migration and invasion of EJ and T24 bladder cancer cell and reduce cancer cell proliferation through the induction of reactive oxygen species (ROS)-dependent apoptosis and mitochondrial dysfunction. Further mechanistic studies using western blotting showed that BSeC-PEI-RGD triggered bladder cancer cell apoptosis by activating p38, JNK and p53 and by inactivating AKT and ERK. In summary, this study demonstrates the rational design of polymer-based cancer-targeting nanosystem as carrier of selenadiazole derivative to treat bladder cancer.

Introduction

Bladder cancer is the fourth most common urinary cancer among men, with an incidence of more than 56,390 new cases and 11,170 estimated deaths in the United States in 2014.[1] The treatment and management of advanced urothelial carcinoma of the bladder is a considerable therapeutic challenge.[2] The most common way to cure bladder cancer is intravesical chemotherapy, which involves infusing drugs through the urethra into bladder.[3,4] If the disease has progressed, chemotherapy remains the main treatment before and after surgery.[5,6] Chemotherapy is successful in bladder cancer to some degree, but it has several limitations. The main drawback is that it lacks sufficient selectivity to the neoplasia and the low pH acidic environment in bladder affected antitumor activity of drugs.[7] Advances in drug delivery are needed and nanomedicine in particular holds promise as a mean to improve drug bioavailability and stability in circulation.[8] These therapies make use of the nanoparticles enhanced permeability and stability within tumors, and thus increase the chemotherapeutic does to the tumor tissue, while simultaneously sparing normal tissue from exposure.[9] Improved drug uptake by tumor cells is also an important consideration for bioavailability.[10,11]

Selenium (Se) is an essential trace element for human life and its important role has been known for years. Se can be divided into two basic chemical forms: organic Se and inorganic Se.[12,13] Se is a promising anti-cancer agent because in cell culture, inorganic Se compounds can induce single-strand breaks in DNA and lead to necrosis. Synthetic organoselenium compounds have also been considered effective and may be chemopreventive agents.[14-21] Organoselenium compounds are Se compounds with promising anti-bladder cancer potential. In our previous studies, the synthetic selenadiazole derivative ASDO induced MCF-7 cancer cell death through caspase- and p53- dependent apoptosis.[22] We also found that a selenadiazole derivative could antagonize hyperglycemia-induced drug resistance in cancer cells through the AMPK-mTORC1-p70S6K1 and AMPK-p53 signaling pathways.[23] Another selenadiazole derivative was found to be thioredoxin reductase inhibitor that induced cancer cell apoptosis.[24] All of our previous studies have suggested that Se-containing compounds have potential as anticancer agents and deserve further research. Nevertheless, organoselenium compounds that lack the ability to target specific cells may result in toxicity

[a] Department of Chemistry, Jinan University, Guangzhou 510632, China. Fax: +86 20 85220223; E-mail: tchentf@jnu.edu.cn, tlxlli@jnu.edu.cn
[b] Department of Urology, General Hospital of Guangzhou Military Command of PLA, Guangzhou 510010, China, zengqinsong01@126.com
[c] Department of Applied Biology and Chemical Technology, The Hong Kong Polytechnic University, Hunghom, Kowloon, Hong Kong
[d] Shenzhen Key Laboratory of Food Biological Safety Control, Food Safety and Technology Research Centre, PolyU Shenzhen Research Institute, Shenzhen, PR China
* Corresponding authors.
†Electronic Supplementary Information (ESI) available: Additional UV-vis absorption spectra and cell viability data. See DOI: 10.1039/x0xx00000x

for healthy tissues. Therefore, the anticancer utilization of organoselenium compounds has been difficult due to their low stability and reduced cellular uptake. A cancer-targeted peptide could be linked to nanoparticles through covalent or noncovalent bonds, which would enhance the ability of organoselenium compounds to accumulate in cancer cells, not in normal cells. In summary, our results have suggested that the tripeptide sequence Arg-Gly-Asp (RGD) may be the ideal target peptide.

RGD is short synthetic peptides that is well known for its integrin-binding activity.[25] Integrins are cell adhesion receptors for extracellular matrix (ECM) proteins, immunoglobulins, growth factors, cytokines, and matrix-degrading proteases. Integrins is critical receptor during various cancer stages, including migration invasion, tumor proliferation and progression and metastasis. Due to the expression of integrins in diverse cell types and their function in tumor proliferation, integrins have become a vital therapeutic target.[26-28] Therefore, this study aimed to use the cancer-targeting peptide RGD to increase the functionality of the selenadiazole derivative BSeC (benzo [1, 2, 5] selenadiazole-5-carboxylic acid) and developed the application of BSeC to the treatment of human bladder cancer.

Cationic liposomes can be a good supplement for drug and gene delivery in cancer therapy.[29,30] Many studies have reported that cationic polymer-conjugated macromolecules can improve the inhibitory effect of drugs on tumor cell proliferation.[31,32] In our previous study, Se nanoparticles with exterior chitosan exhibited enhanced selective cellular uptake and anticancer efficacy.[33,34] PEI, another high-molecular-weight polymer that is excellent for this type of application due to its high water-solubility and controllable characteristics, has been widely used as a non-viral cationic vectors for gene transfection.[35-39] Therefore, in this study, we used PEI to link BSeC and the RGD peptide to fabricate a cancer-targeting conjugate. In summary, this study provides a strategy for the rational design of a Se-containing, cancer-targeted theranostic agents to treat human cancer.

Experimental

Materials

Polyethyleneimine (PEI, 10 kDa), thiazolyl blue tetrazolium bromide (MTT), propidium iodide (PI), Hoechst 33342, dihydroethidium (DHE, Beyotime), and the bicinchoninic acid (BCA) kit were purchased from Sigma. The substrate for caspase-3 (Ac-DEVD-AMC), caspase-8 (Ac-IETD-AFC) and caspase-9 (Ac-LEHD-AFC) were purchased from Calbiochem. The mitochondrial dye JC-1 was obtained from Molecular Probes. Ultrapure water supplied by a Milli-Q water purification system was used for all experiments. All other chemicals were analytical grade.

Preparation of BSeC, BSeC-PEI and BSeC-PEI-RGD

4-Carboxyl-o-phenylenediamine was dissolved in an aqueous HCl solution, then, an aqueous solution of SeO2 was added in a dropwise manner. The crude product was stirred for 12 h at 37 °C. The final product was obtained after silica gel column purification and recrystallization.

PEI was conjugated with BSeC by forming an amido linkage using an NHS/EDC reaction system. The excess BSeC, EDC and NHS were removed through a 24-h dialysis.

RGD was linked to BSeC-PEI using SMP as a linker. The crude product was purified via dialysis in Milli-Q water for 48 h until no Se could be detected in the outer solution by ICP-AES analysis.

Characterization of BSeC-PEI-RGD

The sizes and morphologies of BSeC-PEI-RGD were monitored by transmission electron microscopy (TEM, Hitachi H-7650), Zetasizer particle size analysis (Malvern Instruments Limited). The structure of BSeC-PEI-RGD was characterized by fourier transform infrared spectroscopy (FT-IR, Equinox 55), UV-vis spectrophotometer (Carry 5000) and fluorescence spectroscopy.

Cell culture and cell viability by MTT assay

The EJ, T24 and SV-HUC-1 cells used in this study were obtained from American Type Culture Collection (ATCC, Manassas, VA) and grown in Dulbecco's modified Eagle's medium (DMEM), supplemented with 10% fetal bovine serum (FBS), 100 U/ml penicillin and 50 U/ml streptomycin in a humidified incubator with an atmosphere of 5% CO2 at 37 °C. The viability of three types of cells was examined using the MTT assay.[40]

Determination of cellular uptake

The EJ, T24 and SV-HUC-1 cells were seeded in 6-well plates at a density of 4×10^5 cells per well. After 24h, the cells were washed with PBS three times and incubated with non-phenol red DMEM for 2 h. Then, the cells were incubated with 30 μM BSeC-PEI-RGD for different periods of time. Cellular uptake efficiency was determined using ultraviolet microplate reader.

RGD competition assay

The RGD competition assay was performed as described previously.[41] Uptake efficiency was determined in EJ and T24 cells using an ultraviolet microplate reader. The EJ and T24 cells were first treated with the RGD peptide and then incubated with 30 μM BSeC-PEI-RGD for 4 h.

Wound-healing and invasion assays

The wound-healing assay analyzed cell mobility and transwell assay evaluated the potential invasion of cells. The extent of wound closure was observed after 24 h by dyeing the cells with Hoechst 33342 and imaging them with a fluorescence microscope. In the invasion assay, all of the cells were stained using Giemsa stain and counted under an inverted microscope.[42] Three independent repetitions of the experiments were performed.

Flow cytometry analysis

Flow cytometry was used to analyze the cell cycle distribution after the cells were treated with BSeC-PEI-RGD. The proportion of apoptotic cells was determined by quantifying the sub-G1 peak in the cell cycle distribution that analyzed by MultiCycle, as described previously.[43]

Quantification of caspase activity

Caspase activity was measured as previously described.[40] Caspase-specific substrates (Ac-DEVD-AMC for caspase-3, Ac-IETD-AMC for caspase-8 and Ac-LEHD-AMC for caspase-9) were added to cell lysates in 96-well plates. The plates were incubated at 37 °C for 2 h, and caspase activity was quantified by measuring fluorescence intensity.

Measurement of ROS generation

Intracellular reactive oxygen species (ROS) generation was examined by detecting the intensity of DHE fluorescence using a fluorescence microplate reader as previously described.[43]

Evaluation of mitochondrial membrane potential

The mitochondrial membrane potential ($\Delta\psi_m$) was determined using the fluorescent probe JC-1 as previously described .[44] Green JC-1 fluorescence was used as a measure of the change in mitochondrial membrane potential ($\Delta\psi_m$).

Western blotting

The cellular expression level of signal pathway proteins was examined with western blotting.[34] Total cellular protein was obtained from T24 cells after they were treated with different concentrations of BSeC-PEI-RGD for 72 h and incubated with lysis buffer (Beyotime).

Statistical analysis

The experiments were performed at least three times, and results are presented as the mean ± SD. Differences between two groups were analyzed using two-tailed Student's t-test. Statistical analysis was carried out using SPSS program (SPSS Inc., Chicago, IL, USA). Difference with $P < 0.05$ *(*)* or $P < 0.01$ *(**)* were considered statistically significant. One-way analysis of variance (ANOVA) was used to compare multiple groups.

Results and discussion

Rational design, synthesis and stability of BSeC-PEI-RGD

In our previous study, we showed organoselenium compounds high anticancer efficacy, but also cause side-effects if they lack targeting. Therefore, in this study, as shown in **Figure 1A**, a novel cancer-targeting prodrug, BSeC-PEI-RGD, was rationally designed and synthesized BSeC-PEI-RGD consists of the RGD peptide -conjugated to the selenocompound BSeC, using PEI as a linker. BSeC-PEI-RGD was successfully created and characterized by transmission electron microscopy (TEM). As shown in the TEM image in **Figure 1B**, the diameter of BSeC-PEI-RGD was approximately 200 nm, and BSeC-PEI-RGD presented a monodisperse and homogeneous spherical structure. It is possible that, PEI polymer forms nanoparticles in the aqueous solution, with the outer side enveloped by hydrophilic RGD peptide and the hydrophobic BSeC encapsulated inside the nanoparticles. Therefore, the core-shell structure was clearly observed, in which the BSeC-PEI were embedded inside and RGD ligand was grafted onto the outer surface, and thus formed the outer layer. Infrared spectroscopy (IR) was used to characterize the formation process of the BSeC-PEI-RGD nanosystem. As shown in **Figure 1C**, the peaks at 2940 and 1490 cm^{-1} in the spectra of PEI and BSeC-PEI-RGD were assigned to the symmetrical bending vibration of amino groups and the bending vibration of N-H. The peak at 1680 cm^{-1} in the spectra of RGD and BSeC was assigned to the stretching vibration of the carboxy group. In the spectrum of BSeC-PEI-RGD, the presence of two special peaks at 1648 and 1551 cm^{-1}, corresponding to amide bands I and II, confirmed the formation of CO-NH- groups between BSeC, RGD and PEI. As determined by ICP-AES, the drug loading rate of BSeC in the final product was 21%, and the conjugation ratio of RGD to PEI was about 17.8:1 by BCA kit.

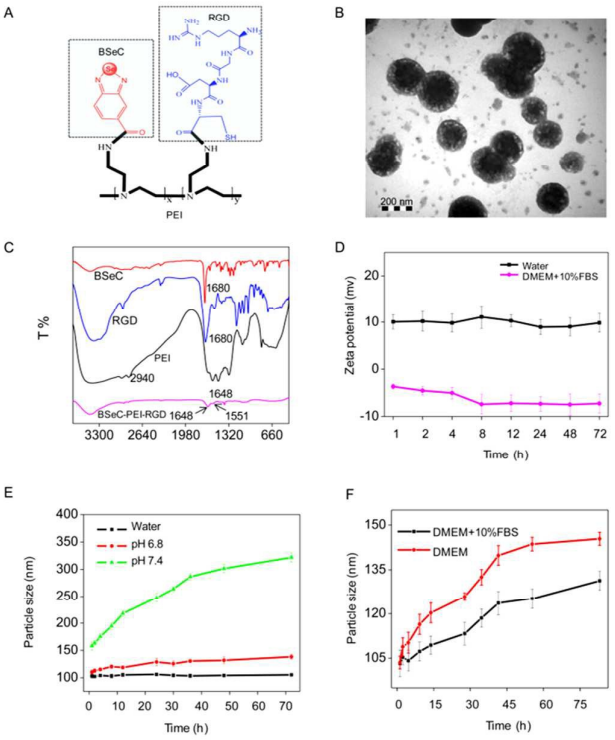

Fig 1. Structure of the BSeC-PEI-RGD complex and the stability of BSeC-PEI-RGD in PBS and DMEM. (A) Structure of the BSeC-PEI-RGD complex, which is composed of the RGD peptide, PEI and BSeC. (B) TEM image of BSeC-PEI-RGD. Scale bars, 200 nm. (C) FT-IR spectra of BSeC, PEI, RGD and BSeC-PEI-RGD. (D) The Zeta potential of BSeC-PEI-RGD in water and DMEM with 10% FBS. (E) The particle size of BSeC-PEI-RGD in PBS solutions that differ in pH. (F) The particle size of BSeC-PEI-RGD in DMEM and DMEM with 10% FBS.

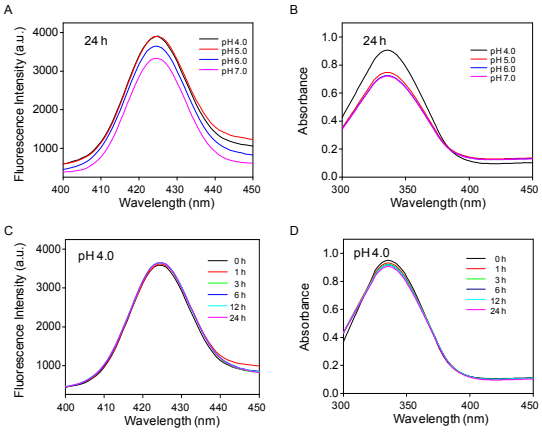

Fig 2. The fluorescence and UV-vis spetra of BSeC-PEI-RGD in different pH PBS solution. (A) The fluorescence spectra of BSeC-PEI-RGD in pH 4.0, pH 5.0, pH 6.0 and pH 7.0 PBS. (B) The UV-vis spectra of BSeC-PEI-RGD in pH 4.0, pH 5.0, pH 6.0 and pH 7.0 PBS. (C) The fluorescence spectra of BSeC-PEI-RGD in pH 4.0 PBS after 24 h. (D) The UV-vis spectra of BSeC-PEI-RGD in pH 4.0 PBS after 24 h.

The stability of BSeC-PEI-RGD is important to maintain it drug activity. To examine the stability of BSeC-PEI-RGD, the Zeta potential and size distribution of BSeC-PEI-RGD were measured. We used a Zetasizer Nano-ZS particle analyzer to examine changes under both aqueous and physiological conditions. As shown in **Figure 1D**, the Zeta potential of BSeC-PEI-RGD decreased in a time-dependent manner in water and DMEM with 10% FBS that simulated physiological environment, whereas the Zeta potential was stable in water and DMEM with 10% FBS. **Figure 1E**, indicates that the size of BSeC-PEI-RGD increased in a time-dependent manner in an aqueous, pH 7.4 PBS solution and increased slowly when placed in a tumor extracellular pH 6.8 PBS solution for 72 h. As shown in **Figure 1F**, the size of BSeC-PEI-RGD remained constant for 72 h, in a solution of DMEM and FBS that simulated physiological conditions. It is possible that some of the negatively-charged proteins in the serum could be adsorbed onto the nanoparticles, which would facilitate the formation of the core-shell structure of the nanosystem and thus enhances its stability.

Low urine pH is an important risk for bladder cancer, that had a marked influence on the antitumor activity of drugs for intravesical chemotherapy in bladder cancer.[45,46] So it is essential to find drugs with high stability in low pH solution. In our study, as shown in **Figure 2A** and **2B**, the fluorescence and UV-vis spectra showed that BSeC-PEI-RGD in different pH solution from pH 4.0 to pH 7.0 have no significant decrease and it was stable in low pH 4.0 solution that simulated bladder-like acidic environment in 24 h. As shown in **Figure 2C** and **2D**, the fluorescence and UV-vis spetra further demonstrated that BSeC-PEI-RGD is stable especially in low pH 4.0 solution as time progressed. Our result suggested that the antitumor activity of BSeC-PEI-RGD could not affected by low pH value.

Cytotoxicity of BSeC, BSeC-PEI and BSeC-PEI-RGD on bladder cells

To demonstrate the anticancer activity and targeting ability of BSeC-PEI-RGD, we first used the MTT assay to assess cell viability. As shown in **Table 1** , the IC_{50} of BSeC-PEI-RGD in EJ and T24 bladder cancer cells was 3.6 μM and 3.1 μM, respectively; these values were much lower than the IC_{50} of BSeC alone (>300 μM). Moreover, BSeC-PEI-RGD demonstrated relatively low cytotoxicity to normal bladder cells, with an IC_{50} value of 6.9 μM. The safety index of the T24 cells also showed that BSeC-PEI-RGD was safe for normal cells. The cell picture of EJ, T24 and SV-HUC-1 treated with different concentration BSeC, BSeC-PEI and BSeC-PEI-RGD showed the result that consistent with the IC50, as shown in **Figure S1.** These results indicate that increasing the functionality of RGD using PEI as the linker significantly enhanced the anticancer efficacy of BSeC, and that BSeC-PEI-RGD exhibits selective anticancer activity. Moreover, as shown in **Figure S2**, PEI and PEI-RGD at less than 8.5 μg/ml and15 μg/ml (corresponding to 10 μM BSeC-PEI-RGD) showed no growth inhibition, with slight growth inhibition observed in cells exposed to 30-240 μg/ml PEI and PEI-RGD (corresponding to 20-160 μM BSeC-PEI-RGD).These results demonstrate that, under the active concentration of BSeC-PEI-RGD (<4 μM), PEI and PEI-RGD showed no significant cytotoxicity toward EJ, T24 and SV-HUC-1 cells.

Table 1 Cytotoxicity and safety index of the selenadiazole and the nanosystem on human bladder cancer cells.

	IC_{50} (μM)			
	EJ	T24	SV-HUC-1[a]	Safe Index[b]
BSeC	397.2±20.4	374.5±21.6	385.7±17.5	1.02
BSeC-PEI	12.5±1.9	13.2±1.4	13.4±1.6	1.02
BSeC-PEI-RGD	3.6±0.4	3.1±0.5	6.9±0.9	2.21

[a] Normal cell
[b] Safe Index = IC_{50} (SV-HUC-1)/IC_{50} (T24)

Cellular uptake of BSeC-PEI-RGD *in Vitro*

Cellular selective uptake can be partially attributed to the different receptor protein of different cells. The RGD peptide located on the surface of BSeC-PEI-RGD can recognize and bind to the integrin receptors overexpressed in bladder cancer cell membranes, enhancing cellular uptake of the nanoparticles through an active targeting process.[41,47] To examine the contribution of integrin receptors to the cellular uptake of BSeC-PEI-RGD, we first should examined the level of expression of the integrin receptor on the cell membrane using western blotting. As shown in **Figure 3A**, integrin receptor

expression levels were significantly higher in the T24 human bladder cancer cells than in the EJ cells. Quantitative analysis of the three cells (**Figure 3B**) confirmed that the expression in T24 cells was significantly higher than that in EJ cells.

To confirm that the different levels of expression of the integrin receptor in the EJ, T24 and SV-HUC-1 cells contributed to the selectivity for cancer cells over normal cells, we quantitatively analyzed and compared the uptake of BSeC and BSeC-PEI-RGD by the EJ, T24 and SV-HUC-1 cells by measuring the ultraviolet fluorescence intensity from the extracellular

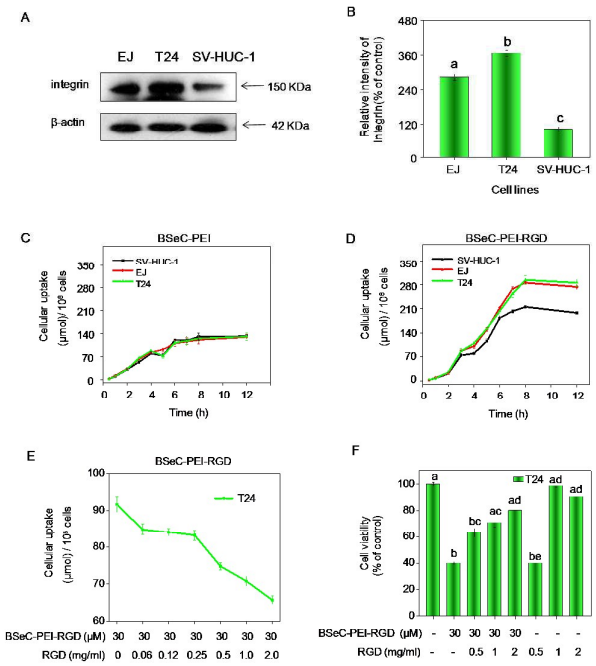

Fig 3. Selective cellular uptake of BSeC-PEI and BSeC-PEI-RGD. (A) Western blot analysis of integrin . (B) Relative intensity of integrin. The results are expressed as percentages of the intensity of the SV-HUC-1 cells. (C) Uptake of 30 μM BSeC by the EJ, T24 and SV-HUC-1 cell lines over 12 h. (D) Uptake of BSeC-PEI-RGD by the EJ, T24 and SV-HUC-1 cell lines, which were exposed to 30 μM BSeC-PEI-RGD for 12 h. (E) Dose-dependent effects of RGD on the cellular uptake of BSeC-PEI-RGD. (F) Cytotoxic effects of BSeC-PEI-RGD on bladder cancer cells and normal cells after a 24-h incubation. Bars with different characters (a, b, c, d and e) are statistically different at $p < 0.05$ level

nanoparticles, as shown in **Figure 3C** and **3D**. The typical absorption peak of BSeC-PEI and BSeC-PEI-RGD was at 335 nm and 340 nm, as shown in the UV-vis spectra (**Figure S3**). The intracellular concentration of BSeC-PEI-RGD was higher than that of BSeC-PEI. The intracellular concentrations were also higher in the T24 cells than in the EJ cells, indicating a positive relationship between cellular uptake and integrin receptor expression. To further demonstrate the positive relationship, we used different concentration of the RGD peptide to block the integrin receptor on T24 cells and analyzed the intracellular drug concentrations. As shown in **Figure 3E** and **3F**, the intracellular concentration of BSeC-PEI-RGD decreased and T24 cell viability increased in dose-dependent manner. The higher integrin expression in the T24 cells allows the T24 cells to absorb more BSeC-PEI-RGD than the EJ cells. Accordingly, less cellular uptake was observed in the SV-HUC-1 cells. Our results suggested that the selectivity of BSeC-PEI-RGD for cancer cells over normal cells is due to the differential expression of integrin, as illustrated using the EJ, T24 and SV-HUC-1 cells.

BSeC-PEI-RGD inhibited bladder cancer cell migration and invasion

Metastasis is very important for the development of tumors, migration and invasion are both necessary for tumor metastasis and growth. Cancer cells are able to migrate from one tissue to another and invade other tissues.[48,49] Wound-healing and transwell assays were performed to assess the anti-invasion and anti-migration capabilities of BSeC-PEI-RGD. As shown in **Figure 4A**, the wound healing assay showed that at a non-toxic concentration of BSeC-PEI-RGD, the EJ and T24 cells displayed notably slower recovery compared to the control cells. The quantitative analysis depicted in **Figure 4B** showed that, the invasion ratio of the T24 cells was lower than that of the EJ cells. These results indicate that BSeC-PEI-RGD inhibited T24 cells invasion more than EJ cells. This result is

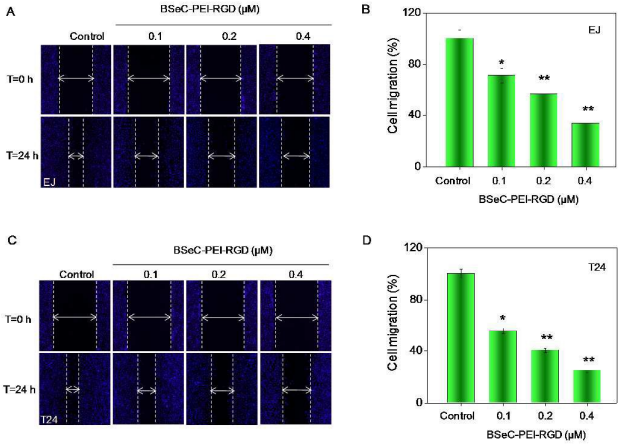

Fig 4. Effects of BSeC-PEI-RGD on EJ and T24 bladder cancer cells migration. (A) The images of EJ cells wound healing assay were acquired at 0 and 24 h after wounding. (B) The results are expressed as percentages of the fluorescence intensity of control EJ cells. (C) The images of T24 cell wound healing assay were acquired at 0 and 24 h after wounding. (D) The results are expressed as percentages of the fluorescence intensity of control T24 cells. The different characters indicate statistically significant difference at *$P<0.05$* and *$P<0.01$*.

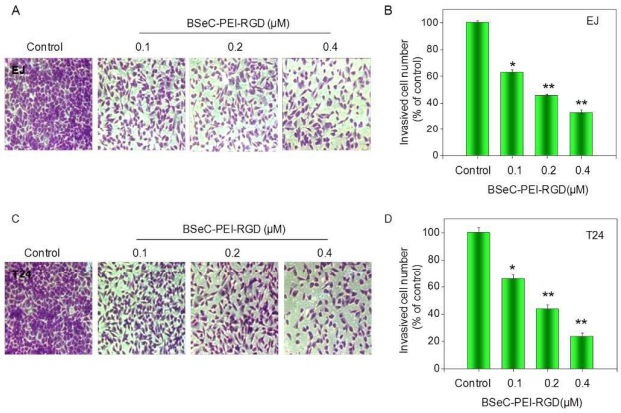

Fig 5. Effects of BSeC-PEI-RGD on EJ and T24 bladder cancer cells invasion. (A) The images depicted the invasion ability of EJ cell. (B) The EJ cells were counted to determine the average number of migrated cells. (C) The images depicted the invasion ability of T24 cell. (D) The T24 cells were counted to determine the average number of migrated cells. The different characters indicate statistically significant difference at **P<0.05* and ***P<0.01*.

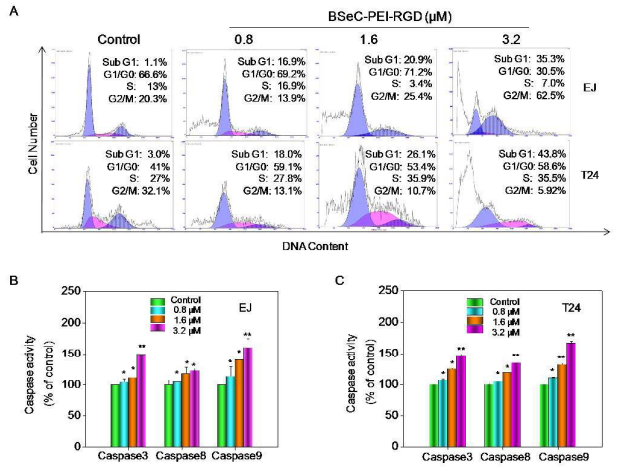

Fig 6. BSeC-PEI-RGD induces the apoptosis of EJ and T24 bladder cancer cells. (A) BSeC-PEI-RGD induces apoptosis in EJ and T24 cells. Apoptotic cells were quantified by measuring the sub-G1 peak. (B) Quantitative analysis of caspase activation triggered in the EJ cell line by BSeC-PEI-RGD. (C) Quantitative analysis of caspase activation triggered in the T24 cell line by BSeC-PEI-RGD.

consistent with the increased cellular uptake in T24 cells compared to EJ cells. Similarly, as shown in **Figure 5A**, the transwell assay showed that the bladder cancer cells exhibited significantly less migration than the controls. The quantitative analysis depicted in **Figure 5B** showed that migration ratio of the T24 cells was lower than that of the EJ cells at 0.2 and 0.4 μM BSeC-PEI-RGD. This result is also consistent with the cellular uptake results. The migration and invasion ratios decreased in a dose-dependent manner. These data suggest that BSeC-PEI-RGD simultaneously inhibit the invasion and migration of the EJ and T24 bladder cancer cell. Moreover, as shown in **Figure S4**, the results of wound-healing assay showed that BSeC-PEI-RGD have no significant inhibition on normal bladder cells SV-HUC-1 migration. The migration ratio of SV-HUC-1 is higher than that of bladder cancer cells EJ and T24. This result is consistent with the MTT assay.

BSeC-PEI-RGD induce apoptosis in bladder cancer cells via caspase activation

Apoptosis is known to play a vital role in a large variety of biological processes, including cell growth, cell replication, embryonic development, changes in cell morphology, and chemical-induced cell death.[50] Moreover, the induction of cell apoptosis may be the vital mechanism underlying the anticancer effects of selenocompounds.[51,52] To further investigate the intracellular mechanism of the antitumor effect of BSeC-PEI-RGD, we performed PI-flow cytometry analyze changes in cell cycle distribution. As reflected in the proportion of sub-G1 cells and cell picture (**Figure 6A**, **Figure S5**), apoptosis was clearly observed in the EJ and T24 cells exposed to BSeC-PEI-RGD. The EJ and T24 cells exposed to different concentrations of BSeC-PEI-RGD exhibited a dose-dependent increase in the sub-G1 cell population, from 16.9% to 35.3% and from 18.0% to 43.8%, respectively. The sub-G1 population

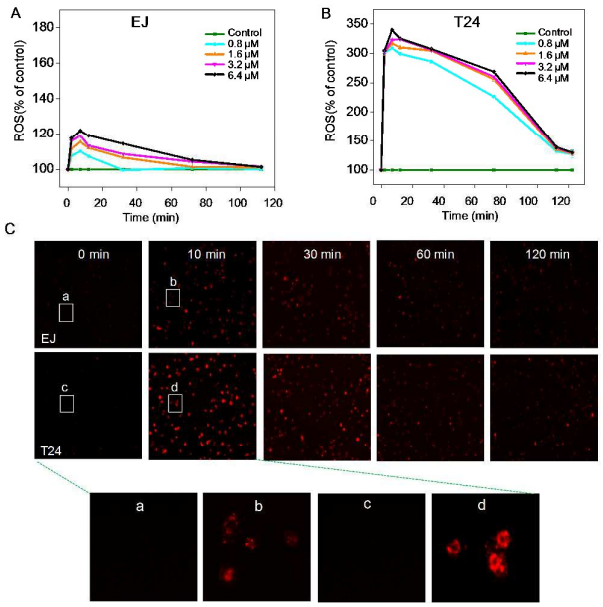

Fig 7. Increase in intracellular ROS generation in EJ and T24 cells with BSeC-PEI-RGD-induced apoptosis. (A) Overproduction of ROS in EJ cells treated with BSeC-PEI-RGD. (B) Overproduction of ROS in T24 cells treated with BSeC-PEI-RGD. (C) ROS generation induced by BSeC-PEI-RGD, as determined by the intensity of DHE fluorescence.

was greater in the T24 cells than in the EJ cells, suggesting that the difference in the anticancer activity of BSeC-PEI-RGD between the T24 and EJ cells was due to the difference in its uptake by these cells.

Caspases are a family of cystein aspartyl proteases, that are very crucial integrators of apoptotic stimuli. Caspase-3 has been implicated as a key mediators of cell apoptosis, while caspase-8 is required to activate downstream caspases and caspase-9 initiates death receptor and mitochondria-mediated apoptotic pathways.[53] To further characterize the mechanisms through which BSeC-PEI-RGD trigger cell apoptosis, the activation status of caspase-3,caspase-8 and caspase-9 were assessed. As shown in **Figure 6B**, BSeC-PEI-RGD notably induced the activation of caspase-3, caspase-8 and caspase-9 in the EJ and T24 cells in a dose-dependent manner. Quantitative analysis of caspase activation based on fluorescence intensity indicated that activation was higher in the T24 cells than in the EJ cells. This result is consistent with the previous results of the MTT assay and the analysis of cellular uptake and apoptosis and indicates that both the intrinsic and the extrinsic pathways contributed to BSeC-PEI-REG-induced apoptosis.

BSeC-PEI-RGD induced apoptosis in T24 and EJ Cells, with increased ROS and mitochondrial dysfunction

Previously studies have suggested that ROS can play a key part in the cancer cell apoptosis induced by organoselenium.[54,55] Accordingly, in this study, the main source of ROS generation was identified using the fluorescent probe DHE. As shown in

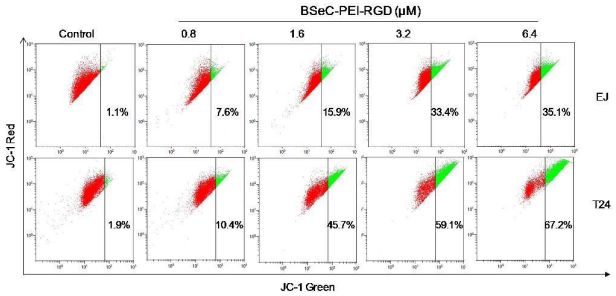

Fig 8. Mitochondrial membrane potential changes (Δψm) induced by BSeC-PEI-RGD. BSeC-PEI-RGD increased mitochondrial membrane potential in EJ and T24 bladder cancer cells. The cells were treated with different concentration of BSeC-PEI-RGD and then analyzed by JC-1 flow cytometry.

Figure 7A, a dose-dependent increase in intracellular ROS generation was observed in EJ cells exposed to different concentrations of BSeC-PEI-RGD in the 2-h incubation. Intracellular ROS generation significantly increased in T24 cells but not in EJ cells, as shown in **Figure 7B**. The increase in ROS generation was greater in the T24 cells compared to the EJ cells. As shown in **Figure 7C**, the fluorescence intensity of ROS generation was higher in the T24 cells treated with BSeC-PEI-RGD than in EJ cells treated with BSeC-PEI-RGD. Exposing the T24 cells to BSeC-PEI-RGD resulted in more damage. This result is in accordance with the previous result that cytotoxicity was higher in the T24 cells than in the EJ cells as well as with the differences in cellular uptake.

Mitochondria play a pivotal part in the regulation of cell life and death by releasing key apoptotic signals of both the extrinsic and intrinsic apoptotic pathways.[56,57] The loss of $\Delta\psi_m$ is connected with the activation of caspases, which initiate apoptotic cascades.[58] We next studied whether the BSeC-PEI-RGD-induced apoptosis involved mitochondrial dysfunction. EJ and T24 cells were treated with different concentrations of BSeC-PEI-RGD for 24 h, and the $\Delta\psi_m$ was examined with flow cytometry, using JC-1 as a fluorescent probe. The fluorescence of the JC-1 dye changes from red to green with a decrease in $\Delta\psi_m$. Therefore, an increase in green fluorescence indicates a loss of Δψm. As shown in **Figure 8**, the BSeC-PEI-RGD-induced loss of Δψm increased in a dose-dependent manner in the treated EJ and T24 cells.The loss of Δψm was significantly larger in the T24 cells than in the EJ cells. This result is

consistent with the previous ROS generation results and shows that BSeC-PEI-RGD exhibits greater anticancer efficacy in T24 cells than EJ cells.

Activation of intracellular apoptotic signalling pathways by BSeC-PEI-RGD

Our previous results have demonstrated the generation of ROS in EJ and T24 cells after treatment with BSeC-PEI-RGD using DHE as a fluorescent probe. An increased concentration of ROS can lead to cell damage and even induce cell apoptosis.[59] To study whether BSeC-PEI-RGD could trigger ROS-mediated apoptosis, we used western blotting to analyze the apoptotic signaling pathway. ERK kinases play a major role in the regulation of cell growth and differentiation, and they are

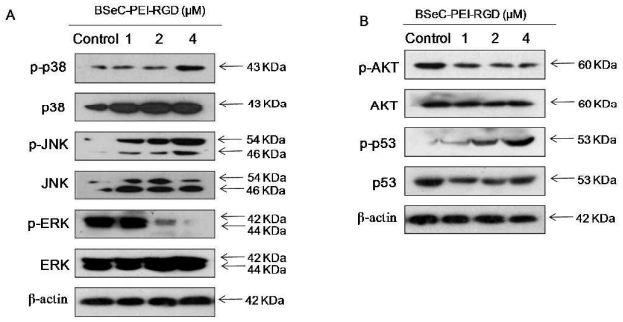

Fig 9. Western blotting analysis of the expression levels of signal proteins after treatment with BSeC-PEI-RGD. (A) p-p38, T-p38, p-JNK, T-JNK, p-ERK, and T-ERK. (B) p-AKT, T-AKT, p-p53,and T-p53. β-actin was used as the loading control.

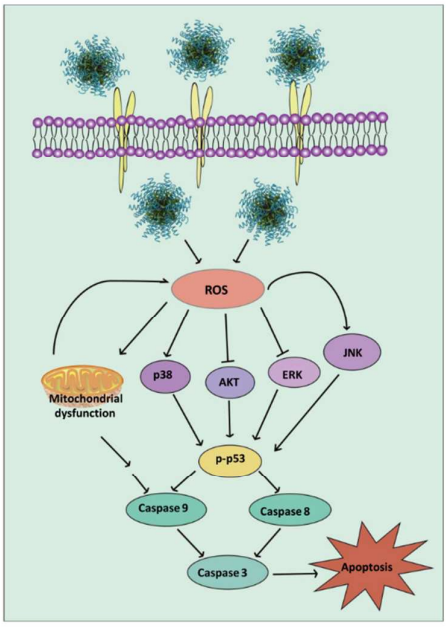

Fig 10. Proposed signaling pathway of apoptosis induced by BSeC-PEI-RGD in T24 cells. The generation of ROS induced by BSeC-PEI-RGD results in AKT and ERK dephosphorylation and activation of p53 pathway, which simultaneously trigger mitochondrial dysfunction.

generally considered prosurvival mediators. AKT kinases have emerged as a critical signaling node in the regulation of cell survival and proliferation, including nutrient metabolism, cell growth, apoptosis and survival in human cancers. As shown in **Figure 9A**, BSeC-PEI-RGD affected the phosphorylation of p38, JNK, ERK, and AKT. Phosphorylation of the pro-apoptotic kinases p38 and JNK displayed a trend toward dose-dependent up-regulation. In contrast, phosphorylation of the anti-apoptotic kinases ERK and AKT was effectively suppressed by BSeC-PEI-RGD. In summary, these results demonstrate that BSeC-PEI-RGD can activate the important parts of p38 and AKT in bladder cancer cells.

In cells, p53 is the product of a suppressor of tumor cell growth and plays a role in mediating cell cycle arrest, DNA repair, and cell apoptosis during the development and malignant progression of tumor.[60-62] As shown in **Figure 9B**, western blotting indicated that the in T24 cells, the total p53 expression level was barely changed by BSeC-PEI-RGD treatmen, but the phosphorylation of p53 was significantly upregulated. Taken together, these results suggest that, the overproduction of ROS induced by BSeC-PEI-RGD may result in AKT and ERK dephosphorylation, which subsequently triggers p53 activation and initiates the apoptotic cascade. ROS act as an upstream mediator for AKT and ERK dephosphorylation, which results in activation of the p53 pathway. AKT and ERK dephosphorylation, which subsequently triggers p53 activation and initiates the apoptotic cascade. ROS act as an upstream mediator for AKT and ERK dephosphorylation, which results in activation of the p53 pathway.The activation of p53 simultaneously enhances the generation of ROS through the induction of mitochondrial dysfunction at the same time. This pathway is summarized in **Figure 10**. Our results demonstrated that BSeC-PEI-RGD strongly induced apoptosis in human bladder cancer cells.

Conclusions

In summary, this study established a novel cancer-targeted prodrug BSeC-PEI-RGD, which consists of the RGD peptide-conjugated to the selenocompound BSeC with the polymer PEI as the linker. In aqueous solution, the PEI polymer forms nanoparticles that are characterized by an outer side that is enveloped by the hydrophilic RGD peptide and that encapsulate the hydrophobic BSeC inside, forming a core-shell nanostructure with enhanced stability in low pH environment that is an important risk for bladder cancer. This rational design effectively enhanced the cell-specific uptake and cyototoxicity of BSeC in human bladder cancer cells and inhibited bladder cancer cell migration and invasion to some extent. BSeC-PEI-RGD displayed enhanced cytotoxicity to cancer cells through the induction of apoptosis involving both intrinsic and extrinsic pathways. Internalized BSeC-PEI-RGD triggered intracellular ROS overproduction and thus activated downstream p53 phosphorylation, promoting cell apoptosis. In summary, this study provides a strategy for the rational design

of Se-containing cancer-targeting nanomedicine to treat human cancers.

Acknowledgements

This work was supported by National High Technology Research and Development Program of China (863 Program, SS2014AA020538), National High-level Personnel of Special Support Program, Science Foundation for Distinguished Young Scholars (S2013050014667) of Guangdong Province, Natural Science Foundation of China, Guangdong Province (2015A0303104) and Guangzhou City (2015A0303104), Foundation for High-level Talents in Higher Education of Guangdong, YangFan Innovative & Entepreneurial Research Team Project (201312H05), Guangdong Special Support Program and Guangdong Frontier and Key Technological Innovation Special Funds.

References

1 R. Siegel, J. Ma, Z. Zou, *et al*., *Ca- Cancer J. Clin.*, 64, (1), 9-29.
2 C. Vale. *J. – Lancet,* 2003**, 361**, (9373), 1927-1934.
3 M. D. Shelley, M. D. Mason, H. Kynaston. *Cancer Treat. Rev.,* 2010**, 36**, (3), 195-205.
4 T. Yoshida, H. Okuyama, M. Nakayama, *et al*., *Cancer Sci.,* 2015**, 106**, (1), 69-77.
5 A. Volpe, M. Racioppi, D. D'Agostino, *et al*., *Urol. Oncol*., 2013**, 31**, (1), 9-16.
6 N. Ismaili, M. Amzerin, A. Flechon. *et al*., *Oncol.,* 2011**, 4**, 35.
7 S. GuhaSarkar, R. Banerjee. *J. Controlled Rrelease.,* 2010**, 148**, (2), 147-59.
8 M. Kanapathipillai, A. Brock, D. E. Ingber. *Adv. Drug Deliv Rev. ,* 2014**, 79-80**, 107-18.
9 Evandro M. Alexandrino, Sandra Ritz, Filippo Marsico, *et al*., *J. Mater. Chem.B.,* 2014**, 2**, 1298-1306.
10 A. Shapira, Y. D. Livney, H. J. Broxterman, *et al., Drug Resist.Updates.,* 2011**, 14**, (3), 150-63.
11 C. Fang, K. Wang, Z. R. Stephen, et al., *ACS Appl Mater Interfaces* 2015**, 7**, (12), 6674-82.
12 M. Brinkman, F. Buntinx, E. Muls, M. P. Zeegers. *Lancet Oncol.,* 2006**, 7**, (9), 766-774.
13 Y. C. Chen , K. S. Prabhu, A. M. Mastro. *Nutrients* 2013**, 5**, (4), 1149-68.
14 J. Y. Liu, Y. Pang, Z. Y. Zhu, *et al.*, *Biomacromolecules* 2013**, 14**, (5), 1627-1636.
15 H. Zeng, W. H. Cheng, L. K. Johnson. *J. Nutr Biochem. ,*2013**, 24**, (5), 776-80.
16 I. Sinha , J. E. Allen , J. T. Pinto, R. Sinha. *Cancer Med.,*2014**, 3**, (2), 252-64.
17 K. El-Bayoumy, R. Sinha. *Mutat. Res. ,*2004**, 551**, (1-2), 181-97.
18 A. dos Santos Edos, E. Hamel, R. Bai , *et al*., *Bioorg. Med. Chem. Lett. ,*2013**, 23**, (16), 4669-73.
19 J. X. de Miranda, O. Andrade Fde, A. Conti, *et al.*, *Trace Elem. Med. Biol. ,* 2014**, 28**, (4), 486-91.
20 P. Ghosh, S. S. Roy, P. Chakraborty, *et al*., Biometals., 2013**, 26**, (1), 61-73.
21 Y. Huang, Y. Luo, W. Zheng, T. Chen. *ACS applied materials & interfaces* 2014**, 6**, (21), 19217-28.
22 T. Chen, Y.-S. Wong, W. Zheng, J. Liu. *Chem. Biol. Interact.,* 2009**, 180**, (1), 54-60.
23 Y. Liu , Y. Luo , X. Li, *et al*., *Chem. Asian J.,*2015**, 10**, (3), 642-52.
24 Q. Xie, Y. Zhou, G. Lan, *et al.*, *Biochem. Biophys. Res. Commun.,* 2014**, 449**, (1), 88-93.
25 F. Wang , Y. Li , Y. Shen, *et al.*, *Int. J. Mol. Sci.,* 2013**, 14**, (7), 13447-62.
26 H. Yang, C. Qin, C. Yu, *et al*., *Adv. Funct. Mater. ,* 2014**, 24**, (12), 1738-1747.
27 L. He, Y. Huang, H. Zhu, *et al.*, *Adv. Funct. Mater. ,* 2014**, 24**, (19), 2754-2763.
28 H. Unal Gulsuner, H. Ceylan, M. O. Guler, *et al.*, *ACS Appl Mater Interfaces.,* 2015**, 7**, (20), 10677-83.
29 J. Ramos , J. Forcada, R. Hidalgo-Alvarez. *Chem. Rev. ,* 2014**, 114**, (1), 367-428.
30 J. Ruesing, O. Rotan, C. Gross-Heitfeld, *et al., J. Mater. Chem. B.,* 2014**, 2**, 4625-4630.
31 F. M. Kievit, O. Veiseh, N. Bhattarai, *et al*., *Adv Funct Mater.,* 2009**, 19**, (14), 2244-2251.
32 J. M. Caster, M. Sethi, S. Kowalczyk, *et al., Nanoscale* 2015**, 7**, (6), 2805-11.
33 B. Yu, Y. Zhang, W. Zheng, *et al*., *Inorg Chem. ,* 2012**, 51**, (16), 8956-63.
34 B. Yu, H. Li, J. Zhang, *et al*., *J. Mater. Chem. B,* 2015**, 3**, (12), 2497-2504.
35 X. Jin, X. Hu, Q. Wang, *et a*l., *Biomaterials,* 2014**, 35**, (10), 3298-308.
36 A. Miguel, M. J. Herrero, L. Sendra, *et al*., *Toxins,* 2014**, 6**, (2), 636-49.
37 Q. Wang, W. Jin, G. Wu, *et al*., *Biomaterials,* 2014**, 35**, (1), 479-88.
38 J. L. Lee, C. W. Lo, C. Inserra, *et al*., *Pharm Res.,* 2014**, 31**, (9), 2354-66.
39 Y. He, Y. Nie, L. Xie, *et al*., *Biomaterials* 2014**, 35**, (5), 1657-66.
40 C. Fan, J. Chen, Y. Wang, *et al*., Chen. *Free Radic Biol Med. ,* 2013**, 65**, 305-16.
41 W. Jiang, Y. Fu, F. Yang, *et al*., *ACS Appl. Mater. Interfaces.,*2014**, 6**, (16), 13738-48.
42 H. Cui, L. Wang, P. H. Gong, *et al*., *Plos One* 2015**, 10**, (4).
43 Y. Huang, L. He, W. Liu, *et al*., *Biomaterials* 2013**, 34**, (29), 7106-16.
44 C. Liu, Z. Liu, M. Li, *et al*.,. *Plos One* 2013**, 8**, (1), e53945.
45 J. Alguacil, R. M. Pfeiffer, L. E. Moore, *et al*., *Eur. J. Epidemiol.,* 2007**, 22**, (2), 91-8.
46 M. E. Wright, D. S. Michaud, P. Pietinen, *et al*., *Cancer causes & control,* 2005**, 16**, (9), 1117-23.
47 Y. P. Yu , Q. Wang, Y. C. Liu, Y. Xie. *Biomaterials* 2014**, 35**, (5), 1667-75.
48 G. P. Gupta, J. Massague. *Cell* 2006**, 127**, (4), 679-95.
49 G. Kroemer, J. Pouyssegur. *Cancer cell* 2008**, 13**, (6), 472-82.
50 G. I. Evan, K. H. Vousden. *Nature* 2001**, 411**, (6835), 342-8.
51 H. Zeng. *Molecules* 2009**, 14**, (3), 1263-78.
52 C. Sanmartin , D. Plano , A. K. Sharma, J. A. Palop. *Int. J. Mol. Sci. ,* 2012**, 13**, (8), 9649-72.
53 M. O. Hengartner. *Nature* 2000**, 407**, (6805), 770-6.
54 J. Y. Su, H. Q. Lai, J. P. Chen, *et al.*, *Plos One* 2013**, 8**, (6).
55 M. Zhou, S. Ji, Z. Wu, *et al*., *Eur. J. Med. Chem.,* 2015**, 96**, 92-7.
56 N. Guaragnella , S. Giannattasio, L. Moro. *Biochem Pharmacol.,* 2014**, 92**, (1), 62-72.
57 V. Gogvadze, S. Orrenius. *Chem. -Biol Interact.,* 2006**, 163**, (1-2), 4-14.
58 B. B. Zhang, D. G. Wang, F. F. Guo, *et al.*, *Fam. Cancer.,* 2015**, 14**, (1), 19-23.

59 T. Chen, Y. S. Wong. *Cell. Mol. Life Sci.,* 2008**, 65**, (17), 2763-75.
60 T. Riley, E. Sontag P. Chen, *et al*., *Nat. Rev. Mol. cell Bio.,* 2008**, 9**, (5), 402-12.
61 C. Lu, W. S. El-Deiry. *Apoptosis,* 2009**, 14**, (4), 597-606.
62 J. D. Amaral, J. M. Xavier, C. J. Steer, *et al*., *Curr Pharm Design,* 2010**, 16**, (22), 2493-2503.

Table of Contents

An integrin-targeting nanosystem as the carrier of selenadiazole derivative to induce ROS-mediated apoptosis in bladder cancer cells, from rational design to action mechanisms

Herein we design a tumor-targeted selenadiazole derivative BSeC and the RGD peptide, which was used as targeting molecule, using a PEI polymer as a linker. The nanoparticles reduced cancer cell proliferation through the induction of ROS-dependent apoptosis and mitochondrial dysfunction. This study demonstrates the rational design of polymer-based cancer-targeting nanosystem as carrier of selenadiazole derivative to treat bladder cancer.